JOURNAL OF GEOPHYSICAL RESEARCH, VOL. 104, NO. A5, PAGES 9963–9973, MAY 1, 1999

A study of solar wind acceleration based on gyrotropic transport equations

Espen Lyngdal Olsen
Harvard-Smithsonian Center for Astrophysics, Cambridge, Massachusetts

Egil Leer
Institute of Theoretical Astrophysics, University of Oslo, Oslo, Norway

Abstract. The gyrotropic transport equations are used to describe an electron-proton solar wind from the 500,000 K level in the upper transition region and out to 30 solar radii. These equations allow for different temperatures parallel and perpendicular to the magnetic field, as well as transport of parallel and perpendicular thermal energy along the field. We find that in models with significant coronal proton heating, the electron temperature is much lower than the proton temperature. The electron gas is collision dominated, the thermal anisotropy is small, and the heat flux is close to a "classical" heat flux. The proton gas is collision dominated in the upper transition region, but the temperature increases rapidly in the inner corona, and the protons become collisionless close to the Sun. The proton heat flux is proportional to the temperature gradient very close to the Sun, but in the extended corona it deviates substantially from a classical heat flux. In models where the proton heating is in the direction perpendicular to the magnetic field, a large perpendicular temperature is produced locally, but the perpendicular thermal motion couples into parallel thermal motion, and the parallel temperature increases outward from the Sun. We obtain a maximum parallel temperature that is comparable to the maximum perpendicular temperature. This result seems to hold for all models where the energy flux necessary to drive high-speed wind is deposited in the corona as heat. The result is not in agreement with UVCS/SOHO observations of the 1216 Å Ly-α line in large coronal holes. These observations are consistent with a much larger random proton motion perpendicular to the magnetic field than parallel to the field. Such anisotropies can be obtained in models of high-speed solar wind if we allow for a significant fraction of the energy flux from the Sun to be in the form of low-frequency, transverse waves. These waves accelerate the solar wind without heating the corona, and they contribute to the line broadening in the direction perpendicular to the magnetic field.

1. Introduction

Since the early works of *Parker* [1958, 1963, 1965], the large majority of the solar wind models has been using the so-called five-moment approximation set of equations. In these models the flow of each species is described by conservation equations for five physical quantities; density, velocity vector (three components), and temperature. The heat flux is taken to be a function of these parameters. In the collision dominated plasma in the inner corona a "classical" heat flux, determined by the temperature and the temperature gradient, may be used, but in the supersonic solar wind, where the gas may be collisionless, it is not clear how the heat flux should be described. The solar wind electrons may be treated as a collision dominated gas to quite large heliocentric distances [cf. *Lie-Svendsen et al.*, 1997], but in solar wind models with significant coronal proton heating the protons become collision-less very close to the sun. In these models we cannot make use of a classical heat flux for the proton gas.

Olsen and Leer [1996a, b] showed that an eight-moment approximation fluid model can be used to obtain a consistent description of the solar wind acceleration region; from the collision-dominated inner corona and well into the supersonic region of the flow. In the eight-moment approximation we solve for the density, flow velocity (three components), temperature, and heat flux density (three components). Eight-moment models, with coronal proton heating, give a rather high coronal proton temperature, due to the small heat flux in the proton gas, and the energy flux that is heating the protons is transferred into gravitational and flow energy flux close to the region where the protons are heated. The eight-moment model may provide a good basis for understanding the energy balance in the corona-solar wind system, but temperature anisotropies are not described in the eight-moment model. Such anisotropies will, most likely, develop in the solar wind emanating from coronal holes, where the proton gas is collision-less rather close to the sun.

By assuming a bi-Maxwellian distribution function we can derive a set of fluid equations with different temperatures parallel and perpendicular to the magnetic field. This set of equations is known as the six-moment approximation (density, velocity (three components), and parallel and perpendicular temperature). Owing to its ability to describe plasma with anisotropic temperatures, the six-moment approximation is better suited, than is the five-moment approximation, in de-

Paper number 1998JA900152.
0148-0227/99/1998JA900152$09.00

scribing the behavior of a plasma in the presence of a strong external magnetic field. (If the magnetic field is strong the plasma motion is along the field and the six-moment reduces to a four-moment description; density, flow speed along the field, and temperature parallel and perpendicular to the field.) However, it is not obvious how heat conduction can be included in this description. As collisions are not frequent enough to make the distribution function isotropic, a classical heat flux may be invalid, but it is not clear how the heat flux should be modified. In earlier work a classical heat flux has been used to describe transport of parallel and perpendicular thermal energy along the field [e.g., *Sandbæk and Leer*, 1995; *Hu et al.*, 1997], but in many studies of solar wind protons, with anisotropic temperature, the proton heat flux has simply been set to zero [e.g., *Leer and Axford*, 1972; *Hollweg and Johnson*, 1988; *McKenzie et al.*, 1995].

A set of equations that yields a consistent description of the heat flow in a plasma with anisotropic temperature may be obtained in the 16-moment fluid model. This description is based on an expansion about a bi-Maxwellian distribution function. The gyrotropic approximation is obtained from the 16-moment equations in the limit of a very strong magnetic field, $B \to \infty$. In this limit the flow is along the magnetic field, the pressure tensor is diagonal, and the heat flow is reduced to transport of parallel and perpendicular thermal energy along the field. The gyrotropic description is therefore a six-moment fluid model [cf. *Demars and Schunk*, 1986; *Gombosi and Nagy*, 1988].

Demars and Schunk [1991] used the time-independent gyrotropic equations to describe the solar wind. Numerical solutions of this set of equations are difficult to obtain, and they had to limit their study to heliocentric distances larger than 28 R_s. (R_s is a solar radius.) Such a study may shed some light on the evolution of the proton velocity distribution function in the supersonic solar wind, but the Coulomb-collision frequency in high-speed streams beyond $r \approx 28\ R_S$ is so small that we may as well treat the protons as a collisionless gas. However, in the corona and inner solar wind, where we go from collision-dominated to collisionless protons, the gyrotropic model can provide a good description of the flow. The heat flux in the model is determined self-consistently, and close to the Sun the magnetic field is so strong that the gyrotropic approximation should be valid.

In this paper we present a gyrotropic fluid description of the outflow of an electron-proton plasma from the very inner corona and out to 30 solar radii. The most important physical properties of the solar wind, such as the mass flux and asymptotic flow speed, are determined by the processes in this region [cf. *Leer and Holzer*, 1980] and the transition from collision-dominated to collisionless flow also occurs here. We solve the time-dependent set of gyrotropic equations and run our numerical code until a steady state solution is obtained. This approach eliminates many of the numerical problems present in time-independent codes.

2. Description of the Model

The gyrotropic approximation fluid description has been adopted from *Demars and Schunk* [1991], and by allowing for time dependence we get the following conservation equations for radially flowing electron-proton gas:

Continuity equation

$$\frac{\partial n}{\partial t} = -\frac{1}{A}\frac{\partial}{\partial r}(nuA) \tag{1}$$

Momentum equation

$$\frac{\partial u}{\partial t} = -u\frac{\partial u}{\partial r} - \frac{k}{m}\left(\frac{\partial T_{e\|}}{\partial r} + \frac{\partial T_{p\|}}{\partial r}\right) - \frac{k(T_{e\|} + T_{p\|})}{nm}\frac{\partial n}{\partial r} - \frac{1}{A}\frac{dA}{dr}\frac{k}{m}[(T_{e\|} - T_{e\perp}) + (T_{p\|} - T_{p\perp})] - \frac{GM_s}{r^2} - \frac{1}{nm}\frac{\partial p_w}{\partial r} + \frac{1}{nm}\left(\frac{\delta M_e}{\delta t} + \frac{\delta M_p}{\delta t}\right) \tag{2}$$

where the thermal forces on electrons and protons add up to zero; $(\delta M_e/\delta t) + (\delta M_p/\delta t) = 0$.

Electron parallel energy equation

$$\frac{\partial T_{e\|}}{\partial t} = -u\frac{\partial T_{e\|}}{\partial r} - 2T_{e\|}\frac{\partial u}{\partial r} - \frac{1}{nk}\frac{\partial q_{e\|}}{\partial r} - \frac{1}{A}\frac{dA}{dr}\frac{q_{e\|}}{nk} + \frac{2}{A}\frac{dA}{dr}\frac{q_{e\perp}}{nk} + \frac{1}{nk}Q_{me\|} + \frac{1}{nk}\frac{\delta E_{e\|}}{\delta t} \tag{3}$$

Electron perpendicular energy equation

$$\frac{\partial T_{e\perp}}{\partial t} = -u\frac{\partial T_{e\perp}}{\partial r} - \frac{1}{A}\frac{dA}{dr}uT_{e\perp} - \frac{1}{nk}\frac{\partial q_{e\perp}}{\partial r} - \frac{2}{A}\frac{dA}{dr}\frac{q_{e\perp}}{nk} + \frac{1}{nk}Q_{me\perp} + \frac{1}{nk}\frac{\delta E_{e\perp}}{\delta t} \tag{4}$$

Heat flow equation for parallel energy in the electrons

$$\frac{\partial q_{e\|}}{\partial t} = -u\frac{\partial q_{e\|}}{\partial r} - 4q_{e\|}\frac{\partial u}{\partial r} - uq_{e\|}\frac{1}{A}\frac{dA}{dr} - 3\frac{k^2nT_{e\|}}{m_e}\frac{\partial T_{e\|}}{\partial r} + \left[\frac{\delta q_{e\|}}{\delta t}\right]' \tag{5}$$

Heat flow equation for perpendicular energy in the electrons

$$\frac{\partial q_{e\perp}}{\partial t} = -u\frac{\partial q_{e\perp}}{\partial r} - 2q_{e\perp}\frac{\partial u}{\partial r} - 2uq_{e\perp}\frac{1}{A}\frac{dA}{dr} - \frac{k^2nT_{e\|}}{m_e}\frac{\partial T_{e\perp}}{\partial r} - \frac{1}{A}\frac{dA}{dr}\frac{k^2nT_{e\perp}}{m_e}(T_{e\|} - T_{e\perp}) + \left[\frac{\delta q_{e\perp}}{\delta t}\right]' \tag{6}$$

Proton parallel energy equation

$$\frac{\partial T_{p\|}}{\partial t} = -u\frac{\partial T_{p\|}}{\partial r} - 2T_{p\|}\frac{\partial u}{\partial r} - \frac{1}{nk}\frac{\partial q_{p\|}}{\partial r} - \frac{1}{A}\frac{dA}{dr}\frac{q_{p\|}}{nk} + \frac{2}{A}\frac{dA}{dr}\frac{q_{p\perp}}{nk} + \frac{1}{nk}Q_{mp\|} + \frac{1}{nk}\frac{\delta E_{p\|}}{\delta t} \tag{7}$$

Proton perpendicular energy equation

$$\frac{\partial T_{p\perp}}{\partial t} = -u\frac{\partial T_{p\perp}}{\partial r} - \frac{1}{A}\frac{dA}{dr}uT_{p\perp} - \frac{1}{nk}\frac{\partial q_{p\perp}}{\partial r} - \frac{2}{A}\frac{dA}{dr}\frac{q_{p\perp}}{nk} + \frac{1}{nk}Q_{mp\perp} + \frac{1}{nk}\frac{\delta E_{p\perp}}{\delta t} \tag{8}$$

Heat flow equation for parallel energy in the protons

$$\frac{\partial q_{p\parallel}}{\partial t} = -u\frac{\partial q_{p\parallel}}{\partial r} - 4q_{p\parallel}\frac{\partial u}{\partial r} - uq_{p\parallel}\frac{1}{A}\frac{dA}{dr} - 3\frac{k^2 n T_{p\parallel}}{m_p}\frac{\partial T_{p\parallel}}{\partial r} + \left[\frac{\delta q_{p\parallel}}{\delta t}\right]' \quad (9)$$

Heat flow equation for perpendicular energy in the protons

$$\frac{\partial q_{p\perp}}{\partial t} = -u\frac{\partial q_{p\perp}}{\partial r} - 2q_{p\perp}\frac{\partial u}{\partial r} - 2uq_{p\perp}\frac{1}{A}\frac{dA}{dr} - \frac{k^2 n T_{p\parallel}}{m_p}\frac{\partial T_{p\perp}}{\partial r} - \frac{1}{A}\frac{dA}{dr}\frac{k^2 n T_{p\perp}}{m_p}(T_{p\parallel} - T_{p\perp}) + \left[\frac{\delta q_{p\perp}}{\delta t}\right]' \quad (10)$$

Here k is Boltzmann's constant, G is the gravitational constant, $m_{e(p)}$ is the electron (proton) mass ($m = m_e + m_p \approx m_p$), and M_s is the solar mass. The n variable is the electron (proton) density, r is heliocentric distance, A is the cross section of the radial flow tube, AB = const, where B is the strength of the (radial) magnetic field, and u is the flow speed (along the magnetic field). $T_\parallel$ and $T_\perp$ are temperatures parallel and perpendicular to the magnetic field. They are related to the total temperature T by

$$T = \tfrac{1}{3}(T_\parallel + 2T_\perp) \quad (11)$$

Similarly, $q_\parallel$ and $q_\perp$ are the heat flux densities along the field of parallel and perpendicular thermal motion. These heat flux densities are related to the total heat flux density q by

$$q = \tfrac{1}{2}(q_\parallel + 2q_\perp) \quad (12)$$

The expressions for the collision terms $\delta M/\delta t$, $\delta E_\parallel/\delta t$, $\delta E_\perp/\delta t$, $[\delta q_\parallel/\delta t]'$, and $[\delta q_\perp/\delta t]'$ were obtained from *Demars and Schunk* [1979] (section 3.2 and appendix). The expressions are very extensive and will not be listed here. We have used the expression for the Coulomb collision frequency ν^{sr} given by *Chodura and Pohl* [1971] (their equation (19)). (Notice that the definition of collision frequency is different in the Chodura and Pohl paper; their collision frequencies must be multiplied by a factor 8/3 [cf. *Demars and Schunk*, 1979].)

We allow for heating of electrons and protons parallel and perpendicular to the magnetic field. In this study the main objective is to study the effects of perpendicular heating. Thus we set $Q_{e(p)\parallel} = 0$. The heating in the perpendicular direction is given by

$$Q_{e\perp} = -\nabla \cdot \mathbf{f}_{me} \quad (13)$$

$$Q_{p\perp} = -\nabla \cdot \mathbf{f}_{mp} \quad (14)$$

where the radial energy flux densities, f_{me} and f_{mp}, are

$$f_{me(p)} = \frac{A_0}{A} f_{me(p)0} \exp\left[-(r - r_0)/H_{me(p)}\right] \quad (15)$$

The electron heating is not crucial for our study, but the numerical integrations turn out to be more stable when some heat is deposited in the electron gas. This is the main reason for allowing for heat input into the electrons (in addition to the collisional heating of the electrons by the protons). There is a force on the plasma associated with the heating process [e.g., *Tu and Marsch*, 1997], but we want to study the effects of perpendicular heating and acceleration separately so the direct acceleration of the flow is neglected. However, we allow for a flux of Alfvén waves that propagate through the solar wind acceleration region without heating the plasma and add all their energy flux to the flow in the form of direct acceleration. The wave force per unit mass on the flow is $-(1/nm)\,\partial p_w/\partial r$, where the "wave pressure" p_w is determined by [e.g., *Hu et al.*, 1997].

$$\frac{\partial p_w}{\partial t} + \frac{1}{A}\frac{\partial}{\partial r}[(u + v_a)Ap_w] + \frac{p_w}{2A}\frac{\partial}{\partial r}(uA) = 0 \quad (16)$$

where v_a is the Alfvén speed. There may be some Alfvén wave energy flux left at the outer boundary, $r = 30\ R_s$, and the wave may be nonlinear inside the outer boundary, but we will not take these effects into account. However, when estimating the asymptotic flow speed we will take into account the wave energy flux that is left at $r = 30\ R_S$.

We consider a rapidly expanding outflow, where the cross section, A, of a radial flow tube increases as [cf. *Kopp and Holzer*, 1976]

$$A = A_0\left(\frac{r}{r_0}\right)^2 \frac{f_{max}e^{(r-r_1)/\sigma} + f_1}{e^{(r-r_1)/\sigma} + 1} \quad (17)$$

where $f_1 = 1 - (f_{max} - 1)e^{(r_0 - r_1)/\sigma}$. We have chosen, quite arbitrarily, $f_{max} = 5$, and we have taken $r_1 = 1.31\ R_S$, and $\sigma = 0.51\ R_s$ [cf. *Munro and Jackson*, 1977].

3. Results

Let us first consider a case where the Alfvén wave energy flux is zero, that is, $p_w = 0$, and the heating in the perpendicular direction, of the protons and electrons, is given by $f_{mp0} = 320\ \mathrm{W\ m^{-2}}$, $H_p = 1\ R_S$ and $f_{me0} = 80\ \mathrm{W\ m^{-2}}$, $H_e = 0.5\ R_S$. The electron density and the temperature at the inner boundary, $r_0 = 1\ R_S$, are $n_0 = 6 \times 10^{13}\ \mathrm{m^{-3}}$ and $T_0 = 5 \times 10^5$ K. (The collisional coupling between electrons and protons is so strong that they have the same temperature at the inner boundary.) We have chosen to fix the electron density at the inner boundary instead of adjusting it to the inward heat flux [e.g., *Withbroe*, 1988; *Wang*, 1993; *Evje and Leer*, 1998]. The results are presented in Figure 1.

In this model we find a solar wind proton flux of $2.6 \times 10^{12}\ \mathrm{m^{-2}\ s^{-1}}$ mapped to the orbit of Earth (Figure 1f). The electron density decreases rapidly in the inner corona and follow an r^{-2} profile in $r > 3\ R_S$ (Figure 1a). This density profile is consistent with an almost constant flow speed outside $r = 3\ R_S$: The flow speed (Figure 1b) increases to 450 km s^{-1} at $r = 3\ R_S$ and at the outer boundary, at $r = 30\ R_S$, the flow speed is 520 km s^{-1}. Figure 1c shows that the electron temperature reaches a maximum of 1.1×10^6 K at $r = 1.3\ R_S$, and it decreases to $T_e = 2.8 \times 10^5$ K at the outer boundary. The electron temperature is isotropic in the corona, but in the solar wind an anisotropy develops, and $(T_{e,\parallel} - T_{e,\perp})/T_e = 0.3$ at the outer boundary. In the corona the electron heat flux is close to the heat flux in a collision-dominated gas. Figure 1d shows that we have $q_{e,\perp} \approx \frac{2}{5}q_e$ and $q_{e,\parallel} \approx \frac{6}{5}q_e$ in this region (where q_e is the classical heat flux density) [cf. *Gombosi and Nagy*, 1988]. In the solar wind we find that $q_{e,\parallel} > 3q_{e,\perp}$.

The proton temperature (Figure 1c) reaches a maximum of 5.5×10^6 K around $r = 2.5\ R_S$. The perpendicular temperature is much larger than the parallel temperature in this region where the protons are heated, but in the solar wind the perpendicular proton temperature decreases as the magnetic field. The parallel proton temperature increases steadily in the solar wind acceleration region and reaches a maximum around

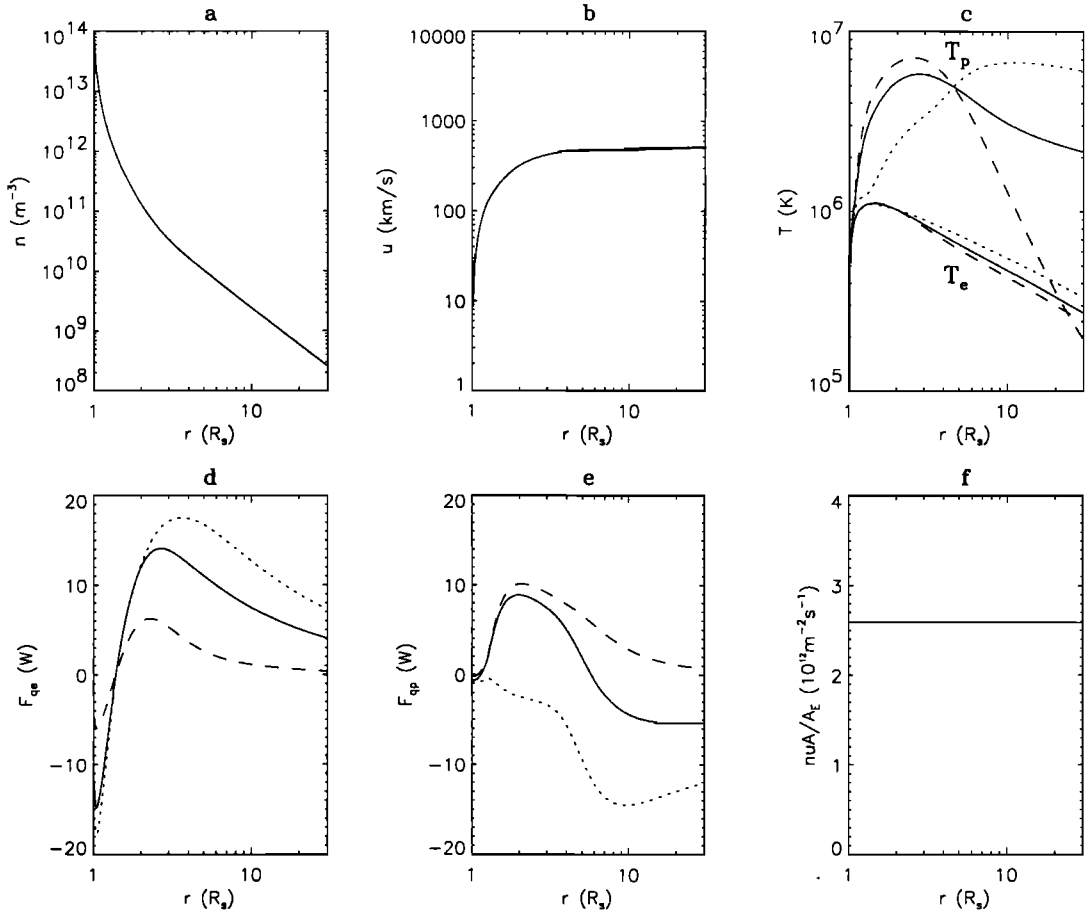

Figure 1. A model with an electron density $n_0 = 6 \times 10^{13}$ m^{-3} at the inner boundary where $T_0 = 5 \times 10^5$ K. The energy flux heating the protons is $f_{mp0} = 320$ W m^{-2}, and the flux heating the electrons is $f_{me0} = 80$ W m^{-2}. The dissipation lengths are $H_p = 1\ R_S$ and $H_e = 0.5\ R_S$. There is no Alfvén wave energy flux in this case, $\langle \delta u_0^2 \rangle^{1/2} = 0$, and $f_{a0} = 0$. In the top row we show the (a) electron density n, (b) the flow speed u, and (c) the electron and proton temperatures, versus heliocentric distance r. The dashed curves give the perpendicular temperatures, $T_\perp$, and the dotted curves show the parallel temperature, $T_\parallel$. The solid curves show $T = \frac{1}{3}(2T_\perp + T_\parallel)$. The bottom row shows the (d) electron and (e) proton heat flux in a radial flow tube with cross section of 1 m^2 at the inner boundary and (f) the (constant) proton flux in a radial flow tube with a cross section of $A_0 = 1$ m^2 at the orbit of Earth. In the plots for the heat fluxes the dashed curve is for the perpendicular heat flux, $q_\perp A/A_0$, and the dotted curve is for the parallel heat flux, $q_\parallel A/A_0$. The solid line in Figures 1d and 1e, is the total heat flux, qA/A_0, where $q = \frac{1}{2}(q_\parallel + 2q_\perp)$.

$r = 8\ R_S$. Notice that the maximum of $T_{p,\parallel}$ is almost as large as the maximum of $T_{p,\perp}$, at $r \approx 2.5\ R_S$. As there is no process, in this model, to significantly reduce the parallel proton temperature in the solar wind, $T_{p,\parallel}$ stays at several million degrees, whereas the perpendicular proton temperature decreases.

In the very inner corona the increase of $T_{p,\parallel}$ is caused by collisional energy transfer, but in the outer corona the divergence of the heat flux density, $q_{p,\perp}$ (Figure 1e), leads to the increase of $T_{p,\parallel}$. (The decrease of $q_{p,\parallel}$ in the corona and in the solar wind adds to the increase of $T_{p,\parallel}$.) The heat flux in the proton gas is very different from the heat flux in a collision-dominated gas, where $q_{p,\parallel} = 3q_{p,\perp}$. In our model we find that $q_{p,\perp} > 0$ and $q_{p,\parallel} < 0$ in most of the region we consider.

This model describes a solar wind with a proton flux that is somewhat higher and a flow speed that is somewhat lower than the observed values in quasi-steady high speed streams. The wind is thermally driven, and almost all the energy flux that is deposited in the corona is lost in the solar wind. However, the energy flux is not transferred directly into flow energy. Part of it is converted into parallel thermal energy. On the basis of the evolution of a collisionless proton distribution function in a rapidly expanding magnetic field we expect to find that a spread in $v_\perp^2$ maps into a similar spread in $v_\parallel^2$, such that $T_{p,\parallel}$ increases when $T_{p,\perp}$ decreases. In earlier work on solar wind models with anisotropic protons this noncollisional coupling of perpendicular thermal motion into parallel thermal motion has not been included.

It may be argued that the large anisotropies in the proton gas, created by perpendicular heating, may lead to excitation of waves, such that there is enhanced coupling within the proton gas. In order to investigate the effects of such an enhanced coupling we have studied models where the proton-proton collision frequency is increased. These models yield a smaller anisotropy than the model in Figure 1, but the results are qualitatively very similar. For instance, in a model where the

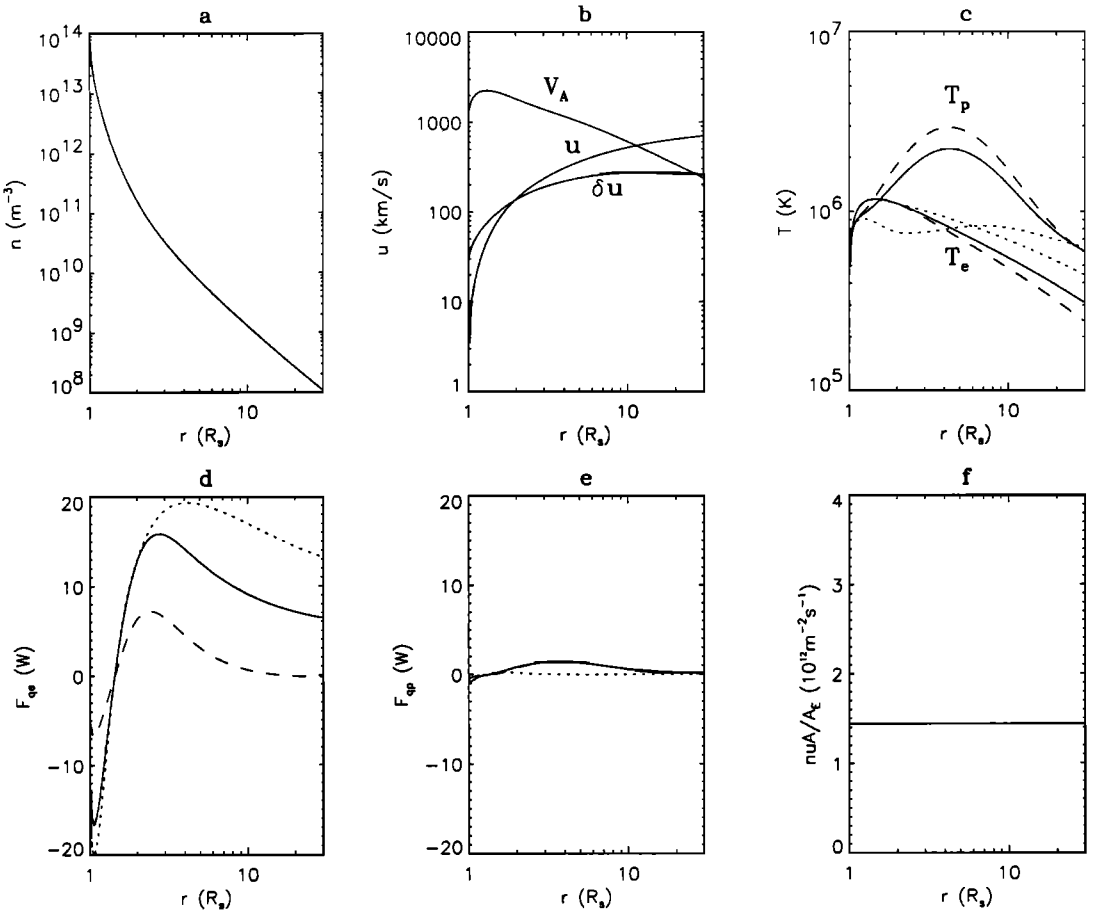

Figure 2. A model with $n_0 = 1 \times 10^{14}$ m^{-3}, $T_0 = 5 \times 10^5$ K, $f_{mp0} = 80$ W m^{-2}, $f_{me0} = 80$ W m^{-2}, and $f_{a0} = 160$ W m^{-2}. The dissipation lengths are $H_p = 1\ R_S$ and $H_e = 0.5\ R_S$, and the Alfvén velocity amplitude at the inner boundary, consistent with the wave energy flux, is $\langle \delta u_0^2 \rangle^{1/2} = 30$ km/s. The panels are arranged as in Figure 1.

proton-proton collision frequency is increased by a factor 30 compared to the Coulomb collision frequency we find a strong coupling in the proton gas in the inner corona; The proton gas is isotropic out to $r = 1.4\ R_S$, where $T_p = 2.8 \times 10^6$ K. The proton heat flux is reduced, but $T_{p,\parallel}$ reaches a maximum of 4.5×10^6 K at $r = 7\ R_S$. The $T_{p,\perp}$ profile in the solar wind is close to the profile shown in Figure 1. We have also investigated models with other boundary conditions, and in all models where the coronal proton heating is strong enough to drive high speed solar wind, we find a parallel proton temperature that increases in the acceleration region and has a maximum that is comparable to the maximum of the perpendicular proton temperature.

It seems that it is virtually impossible to produce a thermally driven high-speed solar wind with a high perpendicular and a much lower parallel proton temperature. Perpendicular heating produces a "pancake" in velocity space, but the evolution of the pancake distribution function into a "sugar-cone," in the solar wind acceleration region, produces a spread in $v_{p,\parallel}^2$ that is comparable with the spread of $v_{p,\perp}^2$, in the pancake. Perpendicular heating could, in principle, produce a smaller spread in $v_{p,\parallel}^2$ provided the perpendicular heating mechanism produces a "doughnut" in velocity space, but this is not likely.

Another possibility for producing the large motion perpendicular to the magnetic field and the small parallel motion that is deduced from the UVCS/Spartan 201 and UVCS/SOHO observations of the 1216 Å Ly-α line in coronal holes [cf. *Kohl et al.*, 1996, 1998] may be to allow for modest proton heating of the corona, and instead of having a purely thermally driven wind, we allow for a flux of low-frequency Alfvén waves that propagates through the corona and "pushes" the solar wind [e.g., *Belcher*, 1971; *Alazraki and Couturier*, 1971; *Hollweg*, 1973]. These waves may carry a substantial fraction of the energy flux that is needed to drive the solar wind, and they will contribute to the broadening of the Ly-α line [cf. *Olsen et al.*, 1994; *Allen et al.*, 1998].

In Figure 2 we show results for a model with Alfvén waves. We have used an electron density of $n_0 = 1 \times 10^{14}$ m^{-3} at the inner boundary, where $T_0 = 500{,}000$ K, and we allow for some heating of the electrons and the proton gas: Both f_{mp0} and f_{me0} are 80 W m^{-2}, and we apply the same damping lengths as in the model shown in Figure 1, namely $H_{mp} = 1\ R_s$ and $H_{me} = 0.5\ R_S$. The Alfvén wave velocity amplitude at the inner boundary is $\delta u_0 = 30$ km s^{-1} and the magnetic field strength is $B_0 = 5 \times 10^{-4} T$, so the Alfvén wave energy flux density at the inner boundary is $f_{a0} \approx 160$ W m^{-2}. Thus, the Alfvén wave energy flux is equal to the mechanical energy flux, $f_{m0} = f_{mp0} + f_{me0} = 160$ W m^{-2}. This corona/solar wind energy input produces a solar wind proton flux, mapped to the orbit of earth, of $(nu)_E = 1.45 \times 10^{12}$ m^{-2} s^{-1} (Figure 2f).

The Alfvén wave energy flux is gradually transferred to the outflowing plasma, as work, and the flow speed increases until all the wave energy flux is transferred to the flow. At the Alfvén point, $r = 11.4\ R_S$, where the flow speed is equal to the local Alfvén speed, approximately 3/8 of the Alfvén wave energy flux is transferred to the flow [e.g., *Hollweg*, 1973]. At the outer boundary some 60% of the energy flux in the wave has been transferred to the expanding plasma, and the flow speed is 700 km s^{-1} (Figure 2b). The wave velocity amplitude is equal to the Alfvén speed inside the outer boundary (Figure 2b), so there will be nonlinear dissipation. This is not included in the model. The wave energy flux, left at the outer boundary, must be transferred to the solar wind: The energy per unit mass in the flow corresponds to an asymptotic flow speed of 840 km s^{-1}.

Figure 2b shows that the wave velocity amplitude, δu, increases quite rapidly away from the Sun, in the inner corona, from 30 km s^{-1} at the inner boundary to 200 km s^{-1} at $r = 3\ R_S$. (In this sub-Alfvénic region the wave energy flux is approximately constant, and the velocity amplitude increases with decreasing mass density, mn, as $\delta u \propto (mn)^{-1/4}$.) From $r = 3\ R_S$ to the outer boundary, at $r = 30\ R_S$, the increase of the wave amplitude is modest: it increases from 200 to 250 km s^{-1}. The wave velocity amplitude corresponds to a proton "temperature" perpendicular to the radial magnetic field of approximately 2.5×10^6 K at $r = 3\ R_S$, and 4×10^6 K at the outer boundary. In this model, with reduced proton heating, the perpendicular proton temperature, $T_{p,\perp}$, has a maximum of 3.5×10^6 K around $r \approx 4\ R_S$, and it decreases rapidly in the solar wind (Figure 2c). There is no significant increase of $T_{p,\parallel}$ in the solar wind acceleration region in this case; the parallel proton temperature is below 1×10^6 K everywhere in the model.

The electron temperature profiles in Figure 2c are similar to the profiles in Figure 1c, but both the temperature and the anisotropy are somewhat larger. The change of the electron temperature is also reflected in the electron heat flux: Figure 2d shows that the parallel heat flux is increased and the perpendicular flux is decreased compared to the heat fluxes shown in Figure 1d.

It should be pointed out that the Alfvén waves are linear ($(\delta u/v_A)^2 < 10\%$) in $r < 7\ R_S$, so our treatment of the Alfvén waves is quite good in this region. In the outer part of our computational domain, $r > 10\ R_S$, where $(\delta u/v_A)^2 > 25\%$, nonlinear damping is important, and the wave energy flux is deposited more rapidly than in our model [e.g., *Ofman and Davila*, 1998]. This will lead to an enhanced flow speed and a reduced electron density. The proton temperature and heat flux profiles will also change. The changes should be small in the corona, out to $r \approx 7\ R_S$, where the nonlinearities are weak. (In this region the magnetic pressure is larger than the thermal pressure and the dynamic pressure, so the gyrotropic equations, obtained in the limit $B \to \infty$, should be valid.)

4. Distribution Functions

In order to derive the gyrotropic transport equations we assume a form of the distribution function [see *Burgers*, 1969; *Demars and Schunk*, 1979]. In a frame that is moving with the flow it is a function of the parallel and perpendicular temperatures, $T_\parallel$ and $T_\perp$, and the parallel and perpendicular heat flux densities, $q_\parallel$ and $q_\perp$:

$$f = f_B(1 + \Psi_B) \tag{18}$$

where f_B is a bi-Maxwellian

$$f_B = \left(\frac{\beta_\perp}{2\pi}\right)\left(\frac{\beta_\parallel}{2\pi}\right)^{1/2} \exp\left(-\tfrac{1}{2}\beta_\perp c_\perp^2 - \tfrac{1}{2}\beta_\parallel c_\parallel^2\right) \tag{19}$$

and the correction factor Ψ_B is

$$\Psi_B = -\frac{\beta_\parallel c_\parallel}{\rho}\left(\beta_\perp q_\perp\left(1 - \tfrac{1}{2}\beta_\perp c_\perp^2\right) + \tfrac{1}{2}\beta_\parallel q_\parallel\left(1 - \tfrac{1}{3}\beta_\parallel c_\parallel^2\right)\right) \tag{20}$$

Here we have introduced $\beta_\perp = m_t/kT_{t,\perp}$ and $\beta_\parallel = m_t/kT_{t,\parallel}$, as well as the mass density of the species we consider, $\rho = m_t n$. The coordinates in velocity space, in the frame moving with the fluid, are $\mathbf{c}_\parallel$ and $\mathbf{c}_\perp$. (Notice that this distribution function reduces to an eight-moment distribution in the isotropic case, where $T_\parallel = T_\perp = T$, $q_\parallel = \frac{6}{5}q$, and $q_\perp = \frac{2}{5}q$.)

After we have solved the fluid equations and determined temperatures and heat fluxes, the distribution functions for electrons and protons, consistent with the solution, can be found. Figures 3 and 4 show the electron and proton distribution functions at four locations, $r = 2$, 5, 10, and 20 R_S, for the models displayed in Figures 1 and 2, respectively. We have plotted seven isocontours to indicate the shape of the distribution function. The maximum, of the normalized distribution, is at unity, and the contours are at 0.8, 0.6, 0.4, 0.2, 0.1, 0.032, and 0.01.

Let us first consider the distribution functions plotted in Figure 3, that is, for the model (in Figure 1) with no Alfvén waves. The top panels show the electron and the bottom panels show the proton distribution function. The electron distribution function in the corona, at $r = 2\ R_S$, is close to an isotropic Maxwellian, in spite of the fact that the electrons are heated only in the perpendicular direction. The electrons collide so frequently in this region that anisotropies do not develop. At $r = 5\ R_S$ we see that an outward "tail" begins to form, and at $r = 10\ R_S$ and at 20 R_S the tail is more pronounced. The skewness of the distribution function corresponds to an electron heat flux that is comparable to a classical heat flux.

The proton distribution function is far from being a Maxwellian, so we must conclude that the collisional interaction in the proton gas is weak. The evolution of the proton distribution function should therefore be determined by the heating perpendicular to the field, and the motion of the protons in the solar gravitational field, the (weak) polarization electric field, and the expanding magnetic field geometry. Figure 3 shows that already at $r = 2\ R_S$ the proton distribution function is very anisotropic. The perpendicular heating produces a width in the perpendicular direction that is much larger than the width along the magnetic field; we have that $T_{p,\perp}/T_{p,\parallel} = 3.5$ at $r = 2\ R_S$. At 5 R_S the parallel and perpendicular widths are comparable, the core is almost isotropic, and we have that $T_{p,\perp}/T_{p,\parallel} = 1.0$. As there is heating also inside $r = 2\ R_S$, and collisions are rather infrequent, the energetic protons form a wide cone at $r = 2\ R_S$. The pitch angle of the energetic protons decreases outwards from the Sun. Figure 3 shows that the cone in velocity space (that follows the isocontours) has an opening angle, α, given by $tg(\alpha) \approx 0.4$, 0.2, and 0.1 at $r =$ 5, 10, and 20 R_S. Because of perpendicular heating $T_{p,\perp}$ stays high out to $r \approx 5\ R_S$, but beyond this distance the heating is small and there is an adiabatic falloff, $T_{p,\perp} \propto r^{-2}$.

The evolution of the proton distribution function can be viewed as a geometric effect, where the perpendicular velocity vectors in the corona are mapped into vectors with a larger parallel component in the solar wind. Therefore the flow speed

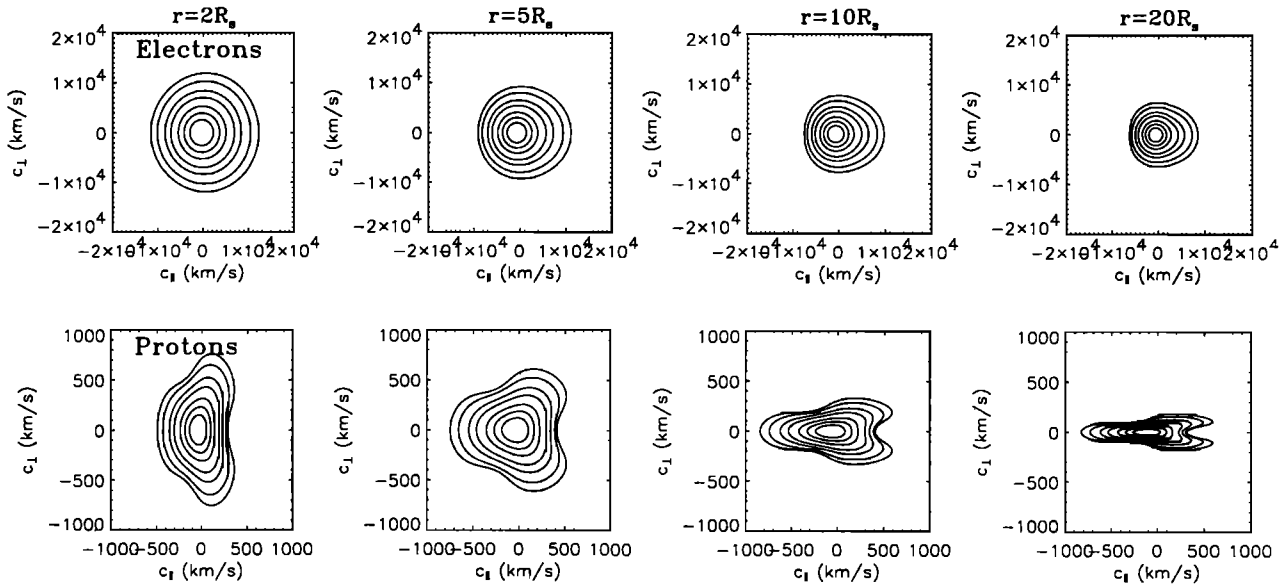

Figure 3. Electron velocity distribution function (top row) and the proton velocity distribution function (bottom row) for the model shown in Figure 1, at r = 2, 5, 10, and 20 R_S (cf. equations (18)–(20)). The horizontal axis is along the radial magnetic field. The distribution functions are normalized such that the maximum is at unity, and the isocontours are at 0.8, 0.6, 0.4, 0.2, 0.1, 0.032, and 0.01.

may increase in this region, and the large spread in perpendicular velocity is mapped into a large spread in parallel velocity. Figure 3 shows that the distribution function is "stretched" significantly in the parallel direction at r = 10 R_S and at r = 20 R_S. As there is no acceleration of the protons parallel to the magnetic field, there is no mechanism that can reduce the width of the distribution function in this direction.

The proton distribution function in Figure 3 has a "core" that stays fairly "round," and the more energetic part of the distribution evolves like "test particles" in an expanding magnetic field. Most of the particles are in the core, and this part does not deviate too much from a bi-Maxwellian. If we consider particles with energy much higher than the local escape energy, such that their kinetic energy is approximately constant, their pitch angle α is given by

$$tg(\alpha) = \left(\frac{B}{B_1 - B}\right)^{1/2} \tag{21}$$

where B_1 is the field strength at the point where the particles "mirror" in the field. (In the inner corona the change of the kinetic energy must be taken into account.) In the solar wind acceleration region, where the magnetic field strength de-

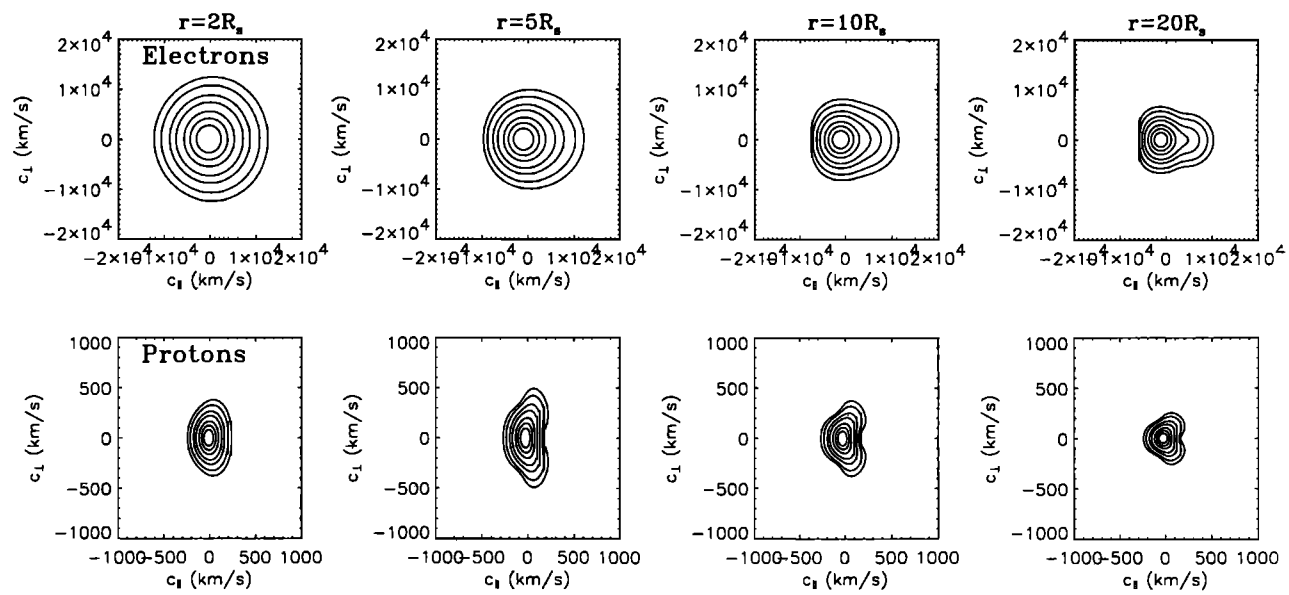

Figure 4. Similar to Figure 3 but shows electron and proton distribution functions for the model displayed in Figure 2.

creases as r^{-2}, the pitch angle decreases as $tg(\alpha) \propto r^{-1}$. This expression agrees quite well with the evolution of the pitch angle for energetic protons seen in Figure 3.

The proton distribution function for the model with Alfvén waves (cf. Figure 2) is presented in Figure 4. In this case the proton heating is reduced, and half of the energy flux that is deposited in the corona/solar wind is in the form of Alfvén waves. The Alfvén wave energy flux is deposited as "work" on the flow. The energy flux that is added as heat (in the perpendicular direction) is split evenly between electrons and protons. The energy flux deposited as heat in the electron gas is the same as for the model in Figure 1.

Let us first consider the electron distribution function: Figure 4, upper panels, show that the electrons in the corona, at $r = 2\ R_S$, are close to an isotropic Maxwellian, and that a tail is formed in the solar wind. As the solar wind electron (proton) flux is smaller in this case than in the model in Figure 1 and the flow speed is larger in $r > 5\ R_S$, the electron density is lower, the temperature is slightly higher, and the collisional coupling is weaker. This results in a more pronounced tail than the electron tail seen in Figure 3, but we find that the electron heat flux is comparable to a classical heat flux also in this model.

The perpendicular proton heating is quite modest, but it produces a fairly high temperature maximum, $T_{p,\perp} \approx 3.5 \times 10^6$ K, and a maximum in the anisotropy, $T_{p,\perp}/T_{p,\parallel} \approx 4$ around $r = 4\ R_S$. The collisional coupling in the proton gas is weak, and perpendicular motion is transferred into parallel motion in the expanding geometry. As we have seen, this process will normally lead to a spread in velocity space, in the parallel direction, that is comparable to the spread in the perpendicular direction, but the acceleration of the flow by the Alfvén waves leads to an increase of all the velocity vectors in the proton distribution function. Thus the spread in velocity space is reduced. Figure 4 shows that the decrease of the width of the distribution function, due to wave acceleration, balances the increase due to mapping of the anisotropic distribution function in the corona, and $T_{p,\parallel}$ does not increase significantly in the solar wind acceleration region (cf. Figure 2c).

The evolution of the distribution functions shown in Figures 3 and 4 seems quite reasonable, for both the almost collision-dominated electrons and the almost collision-less protons. The electron distribution function is similar to the distribution function found by *Lie-Svendsen et al.* [1997], when they solved a Fokker-Planck equation for "test" electrons in a high-speed solar wind background. The proton distribution function seems to have most of the characteristics of a collisionless proton gas in an expanding geometry.

5. Discussion

In the models presented in Figures 1 and 2 the electrons can (to a good approximation) be treated as a collision dominated gas. This approximation is very good in the inner corona, as well as in the solar wind acceleration region. In the outer solar wind anisotropies may develop in the electron distribution function, but classical transport theory is "good enough" to describe the energy transport in the solar wind electrons. It should be pointed out that the gyrotropic description reduces to an eight-moment model in the collision dominated limit. The thermal force between electrons and protons, in the eight-moment model, is larger than the thermal force found by *Spitzer and Härm* [1953], *Braginskii* [1965], and others. Hence the heat conduction coefficient in the electron gas is too small in the present model. This can be corrected for by reducing the thermal force [e.g., *Olsen et al.*, 1998].

The proton heat flow cannot be approximated using a classical heat flux. Even a modest proton heating leads to a coronal proton temperature of a few million degrees, and the proton gas is collisionless rather close to the Sun. The weak collisional coupling allows for large anisotropies to develop, and if we invoke heating mechanisms that preferentially heat in the direction perpendicular to the magnetic field, a proton distribution function with a large perpendicular thermal motion will be produced. This distribution evolves into a cone in an expanding geometry.

The evolution of the distribution function of the protons, from the inner corona and into the solar wind, may be studied using a kinetic model, but such a study is quite an undertaking when heating and collisions play a role. However, the much simpler gyrotropic transport equations seem to describe, quite well, the proton gas in the solar wind acceleration region. The gyrotropic model is based on a bi-Maxwellian distribution functions with a small correction term. Products of the correction terms are neglected in the collision term. This should be a quite good approximation as the correction terms are small in the region where collisions play an important role. We would like to mention that a comparison of a kinetic and a gyrotropic description of the polar wind protons, and their interaction with the background O^+ ions, shows that collisions are described, quite accurately, in the gyrotropic model, even in the region where the proton distribution function deviates significantly from a bi-Maxwellian [cf. *Lie-Svendsen and Olsen*, 1998].

The gyrotropic model describes the transfer of perpendicular thermal motion into parallel thermal motion, in the solar wind acceleration region. It is the perpendicular heat flux density, $q_\perp$, that couples the perpendicular and parallel thermal motions. This can be illustrated by considering the protons in the model without Alfvén waves (cf. Figures 1 and 3), where there is a significant increase of the parallel proton temperature with increasing heliocentric distance.

In Figure 5 we show the terms on the RHS of (7)–(10) for the steady state solution presented in Figure 1. The terms in the equation for the parallel proton temperature are plotted in Figure 5a, and the terms in the equation for the perpendicular proton temperature are plotted in Figure 5b. The terms in the equations for $q_{p\parallel}$ and $q_{p\perp}$ vary significantly with heliocentric distance, mainly because of the variation in electron density. In Figures 5c and 5d we have plotted the RHS terms in (9) and (10), divided by the local electron density. In the figures we have used I, II, III, IV, V, and VI to indicate the RHS-terms in (7)–(10), numbered from left to right.

In the equation for $T_{p,\perp}$ (Figure 5b) the heating term, $(1/nk)\ Q_{mp\perp}$, dominates out to $r \approx 4\ R_S$. The energy flux from the Sun goes into increasing the enthalpy flux, and the $-(T_{p,\perp}/T_p)(r/A)(dA/dr)$ term balances the heating term in the region $1.4\ R_S < r < 3.5\ R_S$. In the region beyond $r \approx 5\ R_S$, where heating ceases to be important, $T_{p,\perp}$ decreases, and $-u(\partial T_{p,\perp}/\partial r) - T_{p,\perp}u(1/A)(dA/dr) \approx 0$. Notice that some of the perpendicular heat input goes into generating the perpendicular heat flux, $q_{p,\perp}$. This heat flux plays an important role in the equation for $T_{p,\parallel}$ (Figure 5a). In the very inner corona the collisional coupling in the proton gas is important, but in most of the region out to $r \approx 5\ R_S$, where $T_{p,\parallel}$ reaches 5×10^6 K, it is the $(2/A)(dA/dr)(q_{p,\perp}/nk)$ term (V) that determines the parallel proton temperature. But how is $q_{p,\perp}$ determined?

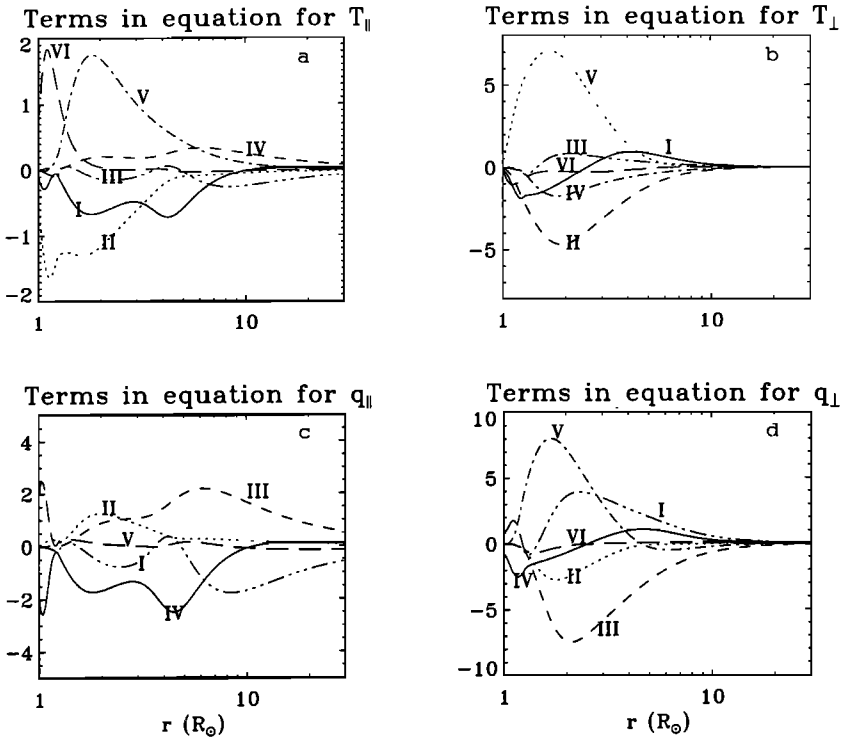

Figure 5. The different terms (measured in 10^3 K/s) in the equations for $T_{p\parallel}$ and $T_{p\perp}$, and the terms in the equations for $q_{p\parallel}$ and $q_{p\perp}$ versus heliocentric distance, for the steady state model presented in Figure 1. The terms in the equations for $q_{p\parallel}$ and $q_{p\perp}$ are divided by the local electron density, n, and they are therefore measured in units of 10^{-15} Wm/s. (a) Terms in equation for $T_{p\parallel}$: I, $-u(\partial T_{p\parallel}/\partial r)$; II, $-[2T_{p\parallel}(\partial u/\partial r)]$; III, $-[(1/nk)(\partial q_{p\parallel}/\partial r)]$; IV, $-[(1/A)(dA/dr)(q_{p\parallel}/nk)]$; V, $(2/A)(dA/dr)(q_{p\perp}/nk)$; VI, $(1/nk)(\delta E_{p\parallel}/\delta t)$. (b) Terms in equation for $T_{p\perp}$: I, $-[u(\partial T_{p\perp}\partial r)]$; II, $-[(1/A)(dA/dr)uT_{p\perp}]$; III, $-[(1/nk)(\partial q_{p\perp}/\partial r)]$; IV, $-[(2/A)(dA/dr)(q_{p\perp}/nk)]$; V, $(1/nk)Q_{me\perp}$; VI, $(1/nk)(\delta E_{p\perp}/\delta t)$. (c) Terms in equation for $q_{p\parallel}$: I, $-[u(\partial q_{p\parallel}/\partial r)]$; II, $-[4q_{p\parallel}(\partial u/\partial r)]$; III, $-[uq_{p\parallel}(1/A)(dA/dr)]$; IV, $-[3(k^2nT_{p\parallel}/m_p)(\partial T_{p\parallel}/\partial r)]$; V, $[\delta q_{p\parallel}/\delta t]'$. (d) Terms in equation for $q_{p\perp}$: I, $-[u(\partial q_{p\perp}/\partial r)]$; II, $-[2q_{p\perp}(\partial u/\partial r)]$; III, $-[2uq_{p\perp}(1/A)(dA/dr)]$; IV, $-[(k^2nT_{p\parallel}/m_p)(\partial T_{p\perp}/\partial r)]$; V, $-[(1/A)(dA/dr)(k^2nT_{p\perp}/mp)](T_{p\parallel} - T_{p\perp})$; VI, $[\delta q_{p\perp}/\delta t]'$.

Figure 5d shows the RHS terms in the equation for $q_{p,\perp}$. In most of the heated region the perpendicular heat flux is determined by the temperature anisotropy;

$$u\frac{\partial q_{p,\perp}}{\partial r} + \frac{1}{A}\frac{dA}{dr}\left[2uq_{p,\perp} + nkT_{p,\parallel}\left(\frac{k(T_{p,\parallel} - T_{p,\perp})}{m}\right)\right] \approx 0 \tag{22}$$

As the thermal anisotropy determines the perpendicular heat flux density, $q_{p,\perp}$, and the perpendicular heat flux determines the proton temperature parallel to the magnetic field, the role of the perpendicular heat flux is to couple the perpendicular and parallel thermal motion in the collisionless region.

The terms in the equation for the parallel heat flux density, $q_{p,\parallel}$, are plotted in Figure 5c. Notice that the parallel heat flux does not play a significant role in the thermal coupling within the proton gas.

We do not include a figure, similar to Figure 5, for the model with Alfvén waves. In that case the proton heating is weaker, and the transfer of perpendicular into parallel thermal energy does not lead to a significant increase of the parallel proton temperature. However, that model shows many similarities to observations of the random motions of electrons and protons in large coronal holes [cf. *Kohl et al.*, 1998]. The electron temperature reaches a maximum of 1.2×10^6 K, the proton motion perpendicular to the magnetic field, that is, the sum of thermal motion and wave motion, corresponds to an "effective" proton temperature perpendicular to the magnetic field that increases quite rapidly in the inner corona and reaches $T_{p,\perp,eff} \approx 4 \times 10^6$ K around $r \approx 4\ R_S$. Beyond this point it stays almost constant. The parallel proton temperature stays below 1×10^6 K. In this model the solar wind proton flux, mapped to the orbit of Earth, $(nu)_E = 1.45 \times 10^{12}\ \mathrm{m^{-2}\,s^{-1}}$, is slightly lower than the proton fluxes observed in high speed streams, and the asymptotic flow speed, 840 km $\mathrm{s^{-1}}$, is somewhat higher.

In this study we have used a Kopp-Holzer geometry with $f_{\max} = 5$. We have not carried out a systematic study of different geometries and expansion factors, but in any reasonable model of high-speed wind the protons are collisionless in the corona. Hence the evolution of their distribution function should be similar to the results presented here.

In order to drive high-speed wind a large fraction of the energy flux from the Sun must be deposited in the supersonic region of the flow. Therefore the damping length, $H_{me(p)}$, cannot be too small if we want to produce high-speed wind with coronal heating. Alfvén waves add most of their energy to the supersonic flow, and speed up a thermally driven wind.

6. Summary

We have demonstrated that the gyrotropic transport equations can be used to describe the outflow of an electron-proton

solar wind in large coronal holes. The gyrotropic model allows for anisotropic heating and temperature anisotropies and is much better suited, than the eight-moment model used by *Olsen and Leer* [1996b], to study the solar wind.

The time-independent equations used by *Demars and Schunk* [1991] are difficult to solve in the solar wind acceleration region due to stiffness. An additional difficulty is that the flow goes from subsonic to supersonic. These problems are avoided by making use of the time-dependent equations, and let the solution evolve in time until a steady-state is reached. The collision terms are so complicated that we found it necessary to use an explicit code, so the relaxation process is quite time consuming. This is the main reason that the solutions are obtained for a fixed electron density at an inner boundary, and not for a density that is consistent with the heat flux into the transition region.

The gyrotropic equations seem to describe, reasonably well, the transition from collision dominated to collisionless flow. In models where the energy flux that is needed to drive the high-speed solar wind streams, is deposited in the corona as perpendicular proton heating, we obtain a high perpendicular proton temperature locally. This temperature decreases adiabatically, whereas the proton temperature parallel to the magnetic field increases. The coupling of the perpendicular thermal energy into parallel thermal motion, in the solar wind acceleration region, leads to a larger parallel than perpendicular proton temperature. This is not in agreement with the proton temperatures in large coronal holes, deduced from UVCS/SOHO observations of the 1216 Å Ly-α line by *Kohl et al.* [1998]. They found that the perpendicular proton temperature is higher than the parallel proton temperature. Thus the present study does not support a model of high-speed wind where the only energy input is heating of the inner corona by ion cyclotron waves.

A broader wave spectrum, where part of the energy flux is in the form of lower-frequency Alfvén waves, will accelerate the flow more gradually. The acceleration of the flow leads to a reduction of the parallel temperature, and with extended ion cyclotron heating we can also maintain a rather high perpendicular temperature. Such a temperature profile is in better agreement with the profiles deduced from the Ly-α observations.

Acknowledgments. We would like to thank J. Kohl and Ø. Lie-Svendsen for discussions. This work was supported by NASA grant NAG5-3192 to the Smithsonian Astrophysical Observatory, by the Research Council of Norway (NFR) under contracts 121076/420 and 107781/432 and by NASA grant W-18.786.

Janet G. Luhmann thanks Leon Ofman and Giorgio Einaudi for their assistance in evaluating this paper.

References

Alazraki, G., and P. Couturier, Solar wind acceleration caused by the gradient of Alfvén wave pressure, *Astron. Astrophys.*, *13*, 380–389, 1971.

Allen, L. A., S. R. Habbal, and Y. Q. Hu, Thermal coupling of protons and neutral hydrogen in the fast solar wind, *J. Geophys. Res.*, *103*, 6551–6569, 1998.

Belcher, J. W., Alfvénic wave pressure and the solar wind, *Astrophys. J.*, *168*, 509–524, 1971.

Braginskii, S. I., Transport processes in a plasma, in *Reviews of Plasma Physics*, edited by M. A. Leontovich, vol. 1, pp. 205–311, Consultants Bureau, New York, 1965.

Burgers, J., *Flow Equations for Composite Gasses*, Academic, San Diego, Calif., 1969.

Chodura, R., and F. Pohl, Hydrodynomic equations for anisotropic plasmas in magnetic fields, II, *Plasma Phys.*, *13*, 645–658, 1971.

Demars, H., and R. Schunk, Transport equations for multispecies plasmas based on individual bi-Maxwellian distributions, *J. Phys. D. Appl. Phys.*, *12*, 1051–1077, 1979.

Demars, H., and R. Schunk, Solutions for bi-Maxwellian transport equations for SAR-arc conditions, *Planet. Space Sci.*, *34*, 1335–1348, 1986.

Demars, H., and R. Schunk, Solutions for bi-Maxwellian transport equations for radial solar wind beyond 28 R_s, *Planet. Space Sci.*, *39*, 435–451, 1991.

Evje, H. O., and E. Leer, Heating of the corona and acceleration of high speed solar wind, *Astron. Astrophys.*, *329*, 735–746, 1998.

Gombosi, T., and A. Nagy, Time-dependent polar wind modeling, *Adv. Space Res.*, *8*(8), 59–68, 1988.

Hollweg, J. V., Alfvén waves in a two fluid model of the solar wind, *Astrophys. J.*, *181*, 547–566, 1973.

Hollweg, J. V., and W. Johnson, Transition region, corona, and solar wind in coronal holes: Some two-fluid models, *J. Geophys. Res.*, *93*, 9547–9554, 1988.

Hu, Y., R. Esser, and S. Habbal, A fast solar wind model with anisotropic proton temperature, *J. Geophys. Res.*, *102*, 14,661–14,676, 1997.

Kohl, J. L., L. Strachan, and L. D. Gardner, Measurement of hydrogen velocity distributions in the extended solar corona, *Astrophys. J.*, *465*, L141–L144, 1996.

Kohl, J. L., et al., UVCS/SOHO emperical determination of anisotropic velocity distributions in the solar corona, *Astrophys. J.*, *501*, L127–L131, 1998.

Kopp, R. A., and T. E. Holzer, Dynamics of coronal hole regions, I, Steady polytropic flows with multiple critical points, *Sol. Phys.*, *49*, 43–56, 1976.

Leer, E., and W. Axford, A two-fluid solar wind model with anisotropic proton temperature, *Sol. Phys.*, *23*, 238–250, 1972.

Leer, E., and T. E. Holzer, Energy addition in the solar wind, *J. Geophys. Res.*, *85*, 4681–4688, 1980.

Lie-Svendsen, Ø., and E. L. Olsen, Comparison of kinetic and hydrodynamic descriptions of the proton polar wind in the transition to collisionless flow, *J. Geophys. Res.*, *103*, 4097–4113, 1997.

Lie-Svendsen, Ø., V. H. Hansteen, and E. Leer, Kinetic electrons in high-speed solar wind streams: Formation of high-energy tails, *J. Geophys. Res.*, *102*, 4701–4718, 1997.

McKenzie, J. F., M. Banaszkiewicz, and W. I. Axford, Acceleration of the high speed solar wind, *Astron. Astrophys.*, *303*, L45–L48, 1995.

Munro, R. H., and B. V. Jackson, Physical properties of a polar coronal hole from 2 to 5R_s, *Astrophys. J.*, *213*, 874–886, 1977.

Ofman, L., and J. Davila, Solar wind acceleration by large-amplitude nonlinear waves: Parameter study, *J. Geophys. Res.*, *103*, 23677–23690, 1998.

Olsen, E. L., and E. Leer, An 8-moment approximation two-fluid model of the solar wind, *J. Geophys. Res.*, *101*, 15591–15603, 1996a.

Olsen, E. L., and E. Leer, Thermally driven electron-proton solar wind; 8-moment approximation, *Astrophys. J.*, *462*, 982–996, 1996b.

Olsen, E. L., E. Leer, and T. Holzer, Neutral hydrogen in the solar wind acceleration region, *Astrophys. J.*, *420*, 913–925, 1994.

Olsen, E. L., E. Leer, and Ø. Lie-Svendsen, An eight-moment model parameter study of the solar wind: Dependence on variations in coronal heating, *Astron. Astrophys.*, *338*, 747–755, 1998.

Parker, E. N., Dynamics of the interplanetary gas and magnetic fields, *Astrophys. J.*, *128*, 664–676, 1958.

Parker, E. N., *Interplanetary Dynamical Processes*, Interscience, New York, 1963.

Parker, E. N., Dynamical theory of the solar wind, *Space Sci. Rev.*, *4*, 666–708, 1965.

Sandbæk, Ø., and E. Leer, Coronal heating and solar wind energy balance, *Astrophys. J.*, *454*, 486–498, 1995.

Spitzer, L., and R. Harm, Transport phenomena in a completely ionized gas, *Phys. Rev.*, *89*, 977–981, 1953.

Tu, C.-Y., and E. Marsch, Two-fluid model for heating of the solar corona and acceleration of the solar wind by high-frequency Alfvén waves, *Sol. Phys.*, *171*, 363–391, 1997.

Wang, Y.-M., Flux-tube divergence, coronal heating, and the solar wind, *Astrophys. Lett.*, *410*, L123–L126, 1993.
Withbroe, G. L., The temperature structure, mass, and energy flow in the corona and inner solar wind, *Astrophys. J.*, *325*, 442–467, 1988.

E. Leer, Institute of Theoretical Astrophysics, University of Oslo, P.O. Box 1029, Blindern, N-0315 Oslo, Norway.

E. L. Olsen, Harvard-Smithsonian Center for Astrophysics, 60 Garden Street, MS 50, Cambridge, MA 02138.

(Received September 16, 1998; revised November 23, 1998; accepted November 23, 1998.)